Available at: http://www.ictp.trieste.it/~pub_off IC/98/153

United Nations Educational Scientific and Cultural Organization
and
International Atomic Energy Agency
THE ABDUS SALAM INTERNATIONAL CENTRE FOR THEORETICAL PHYSICS

BOND-VERSUS-SITE DOPING MODELS FOR OFF-CHAIN-DOPED HALDANE-GAP SYSTEM Y_2 Ba Ni O_5

Jizhong Lou
Department of Physics, Peking University, Beijing 100871, People's Republic of China
and
Institute of Theoretical Physics, P.O. Box 2735, Beijing 100080, People's Republic of China,

Shaojin Qin, Zhaobin Su
Institute of Theoretical Physics, P.O. Box 2735, Beijing 100080, People's Republic of China

and

Lu Yu
Institute of Theoretical Physics, P.O. Box 2735, Beijing 100080, People's Republic of China
and
The Abdus Salam International Centre for Theoretical Physics, Trieste, Italy.

Abstract

Using the density matrix renormalization-group technique, we calculate the impurity energy levels for two different effective models of off-chain doping for quasi-one-dimensional Heisenberg chain compound Y_2 Ba Ni O_5: ferromagnetic bond doping and antiferromagnetic site spin-1/2 doping. Thresholds of the impurity strength for the appearance of localized states are found for both models. However, the ground-state and low-energy excitations for weak impurity strength are different for these two models and the difference can be detected by experiments.

MIRAMARE – TRIESTE
September 1998

In the last fifteen years many theoretical and experimental efforts have been devoted to testing Haldane's original conjecture [1] that the excitation spectrum for integer spin Heisenberg antiferromagnetic (AF) chains has a finite energy gap above the ground state while it is gapless for half-integer cases. The experiments on NENP and Y_2 Ba Ni O_5 have shown explicitly the gap's existence. The gap value can also be estimated by numerical studies, e.g., for isotropic spin-1 AF Heisenberg chain, a gap $\Delta \approx 0.41J$ (where J is the exchange integral) has been obtained by density matrix renormalization-group [2], [3] (DMRG) technique as well as by exact diagonalization with proper extrapolation [4]. However, the knowledge of these spin chains is still far from complete, especially regarding the impurity effects. Recently, the interest in the impurity problem has been revived due to the doping experiment performed on the linear chain compound Y_2 Ba Ni O_5 [5], [6]. Several theoretical studies have been carried out to study the doping effect [7–9]. However, the off-chain doping (when Y^{3+} is replaced by Ca^{2+} or Mg^{2+}) has not been fully studied. This is the subject of the present paper.

Y_2 Ba Ni O_5 contains one-dimensional chain structures composed of oxygen octahedra with Ni^{2+} ions at the center. The inelastic-neutron-scattering (INS) experiments on single crystals of this charge transfer insulator show the chains are highly one dimensional with very weak interchain coupling J_2 ($J_2/J \leq 5 \times 10^{-4}$), [10] where J is the intrachain coupling, and the Haldane gap at $\tilde{q} = \pi$ is almost isotropic, so it is an ideal substance to confront experiment. Furthermore, the doping of this compound can be in-chain as well as off-chain. The nonmagnetic Zn^{2+} ions substituting Ni^{2+} will effectively severe the chain and produce free s=1/2 spins at the two ends, which can be explained by the valence bond solid (VBS) model. [11] Though the specific-heat measurements displaying Schottky anomaly [12] seemed to contradict this picture, a recent DMRG numerical study shows this conflict can be resolved by taking into account the chain length distribution. [13] On the other hand, the off-chain substitution of Y^{3+} by Ca^{2+} or Mg^{2+} will induce holes along the chain. The INS experiments show the holes are localized mainly on the oxygen sites within the chains, [5] between the nearest two Ni^{2+} ions. Since the coupling of the two nearby Ni^{2+} ions is mediated by this oxygen, the doping affect can be modeled in two different ways: one is that the coupling of the two Ni^{2+} is modified (bond doping), the other is that an s=1/2 spin will be localized at the oxygen site, and the localized spin will be coupled to the two Ni^{2+} (s=1/2 site doping). The Hamiltonian of these two effective doping models can be written as

$$H_{bd} = J \sum_{i=1}^{N-1} \mathbf{S}_i \cdot \mathbf{S}_{i+1} + J' \mathbf{S_1} \cdot \mathbf{S}_N \tag{1}$$

and

$$H_{sd} = J \sum_{i=1}^{N-1} \mathbf{S}_i \cdot \mathbf{S}_{i+1} + J''(\mathbf{S}_1 \cdot \sigma_0 + \sigma_0 \cdot \mathbf{S}_N), \tag{2}$$

respectively. Here the periodic boundary condition (PBC) is adopted, N is the chain length, $\mathbf{S}$ denotes the s=1 spin; and in Eq.(2) , $\sigma_\mathbf{0}$ represents the s=1/2 impurity , and here we have assumed that the coupling of the two Ni^{2+} ions around the impurity are destroyed completely.

From the site-doping point of view, the induced s=1/2 spin couples antiferromagnetically with Ni^{2+} on both sides of it. Pictorially, the spin direction of the two Ni spins around the impurity site will be antiparallel to the direction of the localized s=1/2 spin, that is, the two s=1 Ni spins tends to be in the same direction. So the effective coupling of the two site will be ferromagnetic instead of antiferromagnetic. Generically, in the Hamiltonian (1), the coupling J' will be negative, while for the site doping model in Hamiltonian (2), J'' will be positive.

Several numerical studies have been carried out for the two Hamiltonians (1) and (2), [7–9,14,17] but nearly all the calculations were done under the assumption that the impurity bond remains antiferromagnetic. In this communication, we use the DMRG algorithm to calculate the energy spectrum for the two doping models (1) and (2), especially for ferromagnetic bond doping model. If J' (negative) is weak enough in Hamiltonian (1), an in-gap bound state is localized around the impurity site. There is a threshold value J'_c, above which there is no in-gap level or corresponding localized state. We also calculate the spectrum for the impurity state for antiferromagnetic J'' in Hamiltonian (2). Combined with previous studies of other authors [14,17], the two Hamiltonians with J' and J'' AFM as well as FM coupling give a complete description for the spin-1 Heisenberg chain doping models. Experimental data may distinguish which of the two models is more appropriate in describing the off-chain doped Y_2 Ba Ni O_5 compound.

The DMRG scheme we used is similar to the one used in Ref. [9]. We keep 250 states up to chain length 50 throughout all the calculation, and the largest truncation error in our calculation is of the order of 10^{-6}. Then the Shanks transformation [4] is used to obtain the final result. This transformation has been proved to be valid for spin-1 Heisenberg chain by several authors [4,8,9], and we can trust the accuracy of this scaling approach. Before presenting the numerical results, a physically intuitive analysis of the two doping models will be useful.

First, for Hamiltonian (1) of the bond doping cases, results in two limiting cases ($J' \to 0^-$ and $J' \to -\infty$) can be obtained within the framework of the VBS picture. When $J' = 0$, the system becomes an open Heisenberg chain, and the ground state will be fourfold degenerate, where the two edge $s = \frac{1}{2}$ spins couple into a singlet and a triplet. The lowest excited state with $S^z_{tot} = 2$ is separated from the ground state by the Haldane gap, and the continuum spectrum starts there. When the impurity bond intensity increases gradually ($\mid J' \mid << J, J' < 0$ in perturbation regime), the two edge spins will tend to form a triplet, while the singlet state will enter the Haldane gap and become an in-gap state between the triplet ground state and the continuum spectrum. The perturbative result obtained by Sørensen and Affleck [7] (SA) is valid also for the negative J' case. On the other hand, for the strong impurity doping strength, $J' \to -\infty$, the two $s = 1$ spins at the ends of the impurity bond cannot be reduced to $s = \frac{1}{2}$ spins anymore. We must consider the reduced four sites model near the impurity bond and write down the effective Hamiltonian as

$$H = J_{eff}\sigma_1 \cdot \mathbf{S}_1 + J'\mathbf{S}_1 \cdot \mathbf{S}_2 + J_{eff}\mathbf{S}_2 \cdot \sigma_2 \ , \tag{3}$$

where $\mathbf{S_1}$ and $\mathbf{S_2}$ are $s = 1$ spins, and $\sigma_\mathbf{1}$ and $\sigma_\mathbf{2}$ are $s = \frac{1}{2}$ spins due to the VBS picture (the remaining

part of the periodic chain can be viewed as a length L - 2 open chain).

In fact, the model Hamiltonian (3) can account for the essential features of the Hamiltonian (1) for all values of J', from positive to negative beyond the assumption that J_{eff} is positive. Its spectrum contains two singlets, four triplets, three quintets and one septet. Out of the ten states, only a few are important to our discussion: the ground state for $J' > 0$ and that for $J' < 0$, the quintets, which are the low excitation states for some values of $J' < 0$. The energy of these states versus the impurity coupling J' (in units of J_{eff}) is shown in Fig. 1.

For the $J' < 0$ case on the left part of Fig. 1, we see that the ground state is a triplet for all J'. When $J' \to -\infty$, the first excited state is a quintet instead of a singlet. This is an interesting phenomenon for the ferromagnetic impurity doping case, that is, there will be a possible energy crossover between the singlet and quintet for larger $|J'|$. Since the energy difference of this quintet to the ground state is nonzero, we can expect either one bound state for small J_{eff} (more if J_{eff} is small enough) or no bound states for larger J_{eff} within the bulk gap $\Delta = 0.41048(2)$. We will show later that for large $|J'|$ there is no such crossover from our DMRG calculation, and there are no in-gap states for long chains. Therefore, J_{eff} is large enough. Since we know very little about J_{eff} at the present stage, it is impossible to conclude which case will occur without more detailed computation.

For $J' > 0$, the AFM doping case on the right part of Fig. 1, only two states are important: the singlet ground state and the first triplet excitation state. For $J' = 0$ and $J' \to \infty$, the energy difference is zero, so the gap state can be expected for both weak and strong impurity bond strength. Detailed numerical results for this case can be found in previous studies. [7–9]

Now we present DMRG results for Hamiltonian (1) with FM bond doping. The dependence of the relative energy of the lowest excited state with respect to the ground state on the impurity bond is shown in Fig. 2. From the figure, we see clearly that a threshold J'_c exists above which the in-gap state disappears. For weaker impurity bond, the impurity level increases linearly with the bond strength, which agrees with SA's perturbative argument [7] for the weak coupling limit. The relation between the splitting of the ground state and the singlet excitations is $\Delta E = -\alpha^2 J'$, where $\Delta E = 0.112J$ for J'=-0.1J, which is also in excellent agreement with the theoretical work for the AFM case [7]. When the impurity bond strength becomes bigger, the energy of the in-gap state deviates from linear and enters the continuum spectrum at last at a critical point for bond strength near $J' = -0.7J$. The simple four-site model based on the VBS picture discussed above shows a crossover between the singlet state (in-gap state for some values of J') and the quintet state, which remains at the bottom of the continuum spectrum. We did not find such a feature in the calculation, so there is no energy crossover taking place, this is due to the interaction between the singlet state and the continuum spectrum, which keeps the singlet state as the lowest-energy excitation state for longer chain length.

The local bond energy $\langle \mathbf{S}_i \cdot \mathbf{S}_{i+1} \rangle_{m^p} - \langle \mathbf{S}_i \cdot \mathbf{S}_{i+1} \rangle_1$- for different impurity bond strengths is presented in Fig. 3 (here m represent the total spin and p is the parity of the state). The $m^p = 2^+$ state corresponds to the one-magnon excitation [15,16]. It changes very little when the impurity bond strength changes from very weak (-0.1J) up to very strong (4.0J)(this is different from the positive J' case, because

for J'=1.0J, this is a two-magnon states [15,16]). On the other hand, the $m^p = 0^+$ state is an edge excitation localized around the impurity bond for weak J'. When J' becomes bigger, this excitation is delocalized and shows a single-magnon-like behavior in the strong coupling region. This is also consistent with the absence of the in-gap impurity states in this region.

We also calculate the ground state and the first excited state (the subgap state) pair correlations of the site nearest to the impurity bond for different J' , that is, $\langle \mathbf{S}_i \cdot \mathbf{S}_{50} \rangle$, which is presented in Fig. 4. For $J' = 0$, the open chain case, we see that for $i > 25$, the pair correlations for the two states are in phase, but for $i < 25$, they are out of phase. This phase difference which keeps the orthogonality of the two states is due to the different coupling of the two chain-end 1/2 spins. In contrast, for strong J', the correlations are almost identical except those i in the middle of the chain where the one-magnon amplitude is the biggest. [15,16] The correlations for the two states are both independent of J' for $i > 25$, while for S^z_{tot}=1, the ground state, the correlations for $i < 25$ will become larger, and for $S^z_{tot} = 0$, the first excited state, the correlation will change its phase when increasing J'. The orthogonality of the two states will mainly come from those sites in the middle of the chain. This also means that the edge excitation (near the impurity bond) when J' is weaker will become a bulk excitation (far away from the impurity bond) when J' is stronger.

Secondly, we analyze the spectrum of Hamiltonian (2). The impurity coupling J'' is positive. Let us reduce the Hamiltonian (2) to a three sites effective Hamiltonian around the impurity $s = 1/2$:

$$H = J_{eff}(\sigma_1 \cdot \sigma_0 + \sigma_0 \cdot \sigma_N). \tag{4}$$

Here $\boldsymbol{\sigma_1}$ and $\boldsymbol{\sigma_N}$ are the effective $s = 1/2$ edge spins from the bulk of the chain, and $\boldsymbol{\sigma_0}$ is the impurity spin. As we analyzed above, here we have $J_{eff} > 0$. In the perturbation regime ($J_{eff} \sim 0$), we know that Hamiltonian (4) has a doublet ground state, a doublet first excited state, and a quartet highest excited state. [7] For the original Hamiltonian (2), as J_{eff} increases, we could see that the doublet ground state will not change, while the two in-gap states given by the reduced Hamiltonian increase linearly with J_{eff}. By DMRG calculation, we find J'' in Eq. (2) has two critical impurity coupling J''_{1c} and J''_{2c}, which correspond to the points where the doublet and the quartet enter the continuum spectrum, respectively.

For the site doping Hamiltonian (2), we consider both the ferromagnetic coupling ($J'' < 0$) and the antiferromagnetic coupling case ($J'' > 0$). The ground state is a quartet for the former while a doublet for the latter. Two in-gap states are found in the weak coupling regime in each of the two cases, and its energy spectrum is shown in Fig. 5. The thresholds where the in-gap state enters the continuum are $J''_{1c} = -0.25J$, $J''_{2c} = -1.4J$ and $J''_{1c} = 0.3J$, $J''_{2c} = 0.5J$ for the ferromagnetic and antiferromagnetic impurity coupling, respectively. These results are consistent with the previous calculation. [7]

In summary, we have considered two kinds of effective models for off-chain doping in a one-dimensional Heisenberg chain using the DMRG algorithm. Thresholds of the impurity bond strength are found for both ferromagnetic bond doping model and antiferromagnetic $s = 1/2$ site doping model. The ground states of the two kinds of effective models are of total spin 1 and total spin 1/2, respec-

tively. The in-gap states that appear for the weak impurity bond are also different for the two models. A singlet impurity state for ferromagnetic bond doping and a doublet along with a quartet for AF site $s = 1/2$ doping. We believe these properties of the spectrum for different effective doping models can be distinguished by experiments. The doped holes in the off-chain doping case can contribute to the transport properties of the Haldane chain systems. This issue was discussed by other authors [17] and is not addressed here.

Acknowledgments

This work was supported by the NSFC and the calculations were supported by the LSEC and CCAST. One of the authors (J.L.) would like to thank Dr. T. Xiang and Dr. X. Wang for useful discussions.

References

[1] F. D. M. Haldane, Phys. Lett. **93A**, 464 (1983); Phys. Rev.Lett. **50**, 1153 (1983).
[2] S. R. White, Phys. Rev. Lett. **69**, 2863 (1992); Phys. Rev. B**48** 10345(1993).
[3] S. R. White and D. A. Huse, Phys. Rev. B **48**, 3844 (1993).
[4] O. Golinelli, Th. Jolicœur and R. Lacaze, Phys. Rev. B**50**, 3037 (1994).
[5] J. F. DiTusa *et al.*, Phys. Rev. Lett. **73**, 1857 (1994).
[6] K. Kojima *et al.*, Phys. Rev. Lett. **74**, 3471 (1995).
[7] E.S. Sørensen and I. Affleck, Phys. Rev. B**51**, 16115 (1995).
[8] Wei Wang, Shaojin Qin, Zhong-Yi Lu, Zhao-bin Su and Lu Yu, Phys. Rev. B**53**, 40 (1996).
[9] Xiaoqun Wang and Steffen Mallwitz, Phys. Rev. B**53**, R492 (1996).
[10] Guangyong Xu *et al.* , Phys. Rev. B**54**, R6827 (1996).
[11] I. Affleck, T. Kennedy, E. H. Lieb and H. Tasaki, Phys. Rev. Lett. **59**, 799 (1987); Commun. Math. Phys. **115**, 477 (1988).
[12] A. P. Ramirez, S-W. Cheong, M. L. Kaplan, Phys. Rev. Lett. **72**, 3108 (1994).
[13] K. Hallberg, C. D. Batista and A. A. Aligia, cond-mat/9709111 (unpublished).
[14] M.Kaburagi and T. Tonegawa, J. Phys. Soc. Jpn. **63**, 420 (1994).
[15] E.S. Sørensen and I. Affleck, Phys.Rev. Lett. **71**, 1633 (1993).
[16] E. S. Sørensen and I. Affleck, Phys. Rev. B**49**, 15771 (1994).
[17] K. Penc and H. Shiba, Phys. Rev. B**52**, R715 (1995); E. Dagotto, J. Riera, A. Sandvik, and A. Moreo, Phys. Rev. Lett. **76**, 1731 (1996).

FIG. 1. The low-energy spectrum of the reduced bond doping Hamiltonian (3).

FIG. 2. The energy spectrum of the bond doping Hamiltonian (1) when the impurity bond is ferromagnetic. The dotted line indicates the Haldane gap of a pure spin-1 Heisenberg chain.

FIG. 3. The local bond energy $\langle \mathbf{S}_i \cdot \mathbf{S}_{i+1} \rangle_{m^p} - \langle \mathbf{S}_i \cdot \mathbf{S}_{i+1} \rangle_{1^-}$ for different ferromagnetic doping bond J', where m^p equals 0^+ and 2^+.

FIG. 4. The pair correlations $\langle \mathbf{S}_i \cdot \mathbf{S}_{50} \rangle$ of the ferromagnetic bond doping for the ground state 1^- and the first excitation state 0^+.

FIG. 5. The energy spectrum of the site doping Hamiltonian (2). The dotted line indicates the Haldane gap of the pure spin-1 Heisenberg chain.

Lou *et.al.* Fig.5 PRB

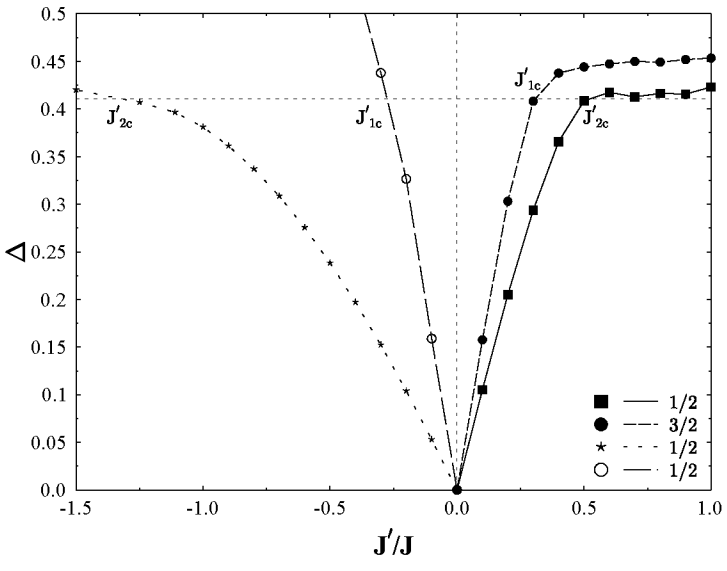

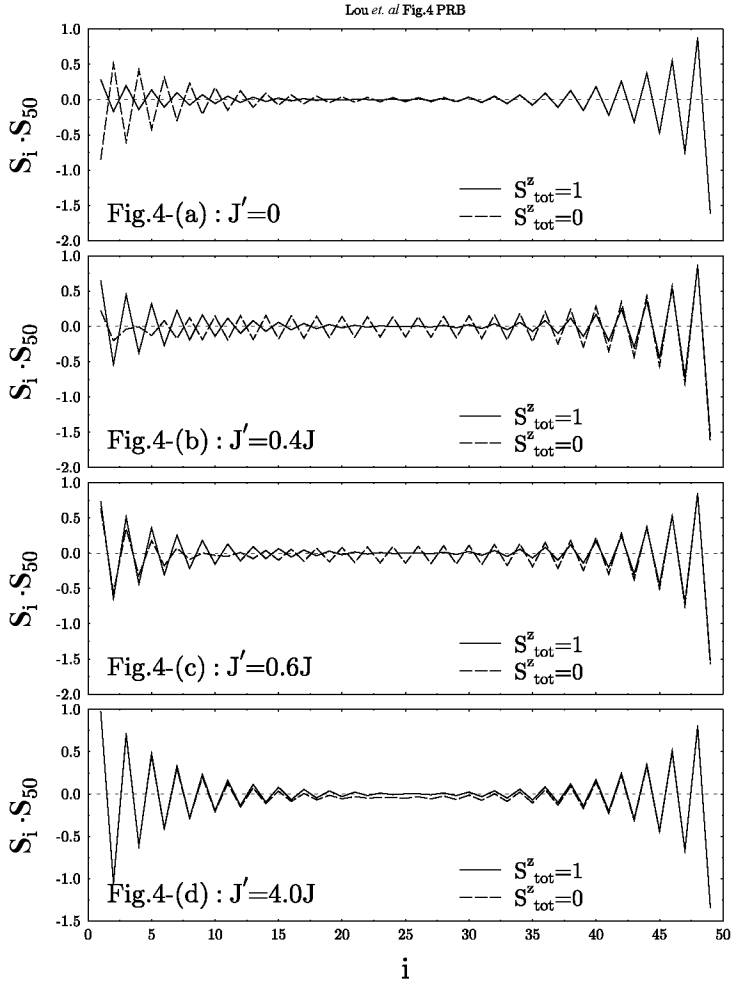
Lou et. al Fig.4 PRB
$S_i \cdot S_{50}$
Fig.4-(a) : J′=0
Fig.4-(b) : J′=0.4J
Fig.4-(c) : J′=0.6J
Fig.4-(d) : J′=4.0J
S^z_{tot}=1
S^z_{tot}=0
i

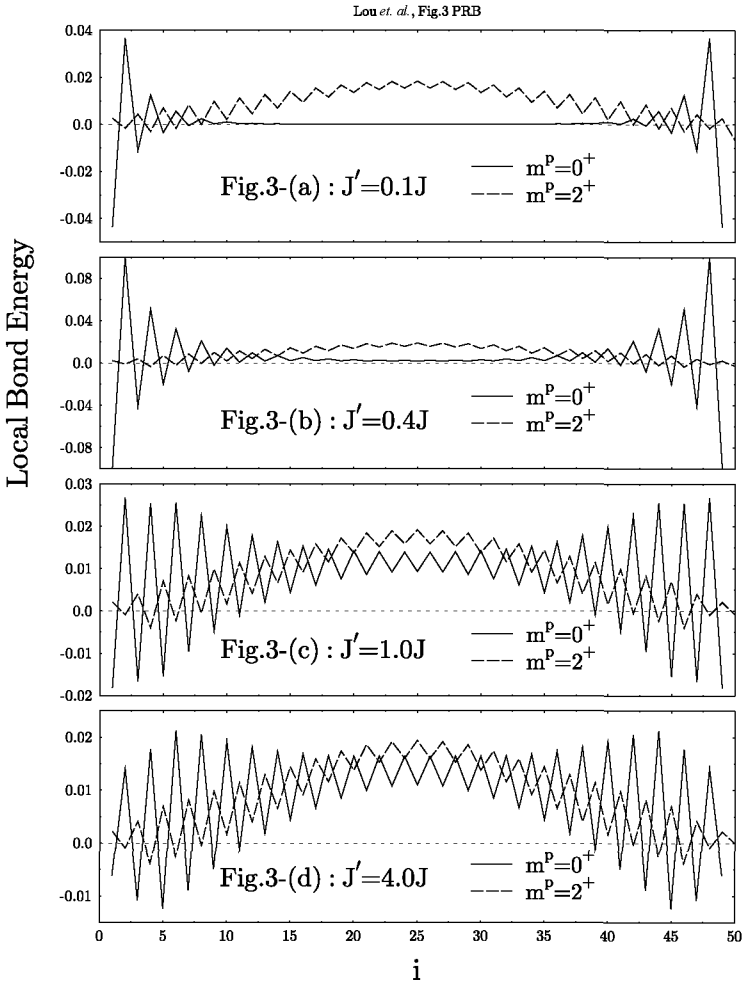
Lou et. al., Fig.3 PRB
Local Bond Energy
i
Fig.3-(a) : J′=0.1J
Fig.3-(b) : J′=0.4J
Fig.3-(c) : J′=1.0J
Fig.3-(d) : J′=4.0J
m^p=0^+
m^p=2^+

Lou *et. al* Fig.2 PRB

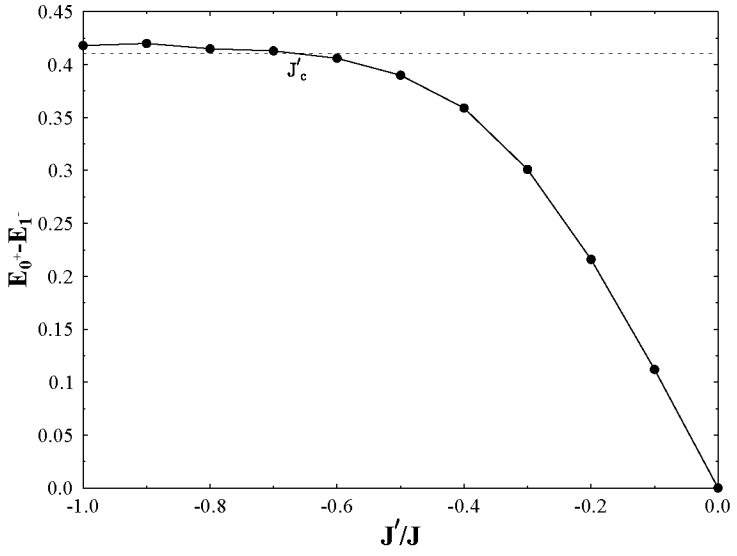

Lou et. al. Fig.1 PRB